




# Forced dynamic analysis of functionally graded beams under harmonic moving loads on elastic foundation with the finite element method

Amine Zemri<sup>a</sup>, Ismail Mechab<sup>b</sup>

<sup>a</sup> University of Relizane,  
Civil Engineering and Public Works Department,  
Relizane, People's Democratic Republic of Algeria;  
University of Sidi Bel Abbès,  
Civil Engineering and Environmental Laboratory,  
Sidi Bel Abbès, People's Democratic Republic of Algeria,  
e-mail: amine.btp@hotmail.fr, **corresponding author**,  
ORCID iD:  <https://orcid.org/0000-0001-7995-6248>

<sup>b</sup> University of Sidi Bel Abbès,  
Civil Engineering and Public Works Department,  
Statistics and Stochastic Processes Laboratory,  
Sidi Bel Abbès, People's Democratic Republic of Algeria,  
e-mail: ismail.mechab@gmail.com,  
ORCID iD:  <https://orcid.org/0009-0004-4922-6980>

 <https://doi.org/10.5937/vojtehg72-50200>

FIELD: mechanical engineering, materials

ARTICLE TYPE: original scientific paper

## Abstract:

*Introduction/purpose:* This paper presents a numerical study of the forced dynamic behavior of a functionally graded beam subjected to a harmonically varying transversely concentrated moving force using a higher-order shear deformation theory.

*Methods:* The governing equations are derived using Hamilton's principle. These equations are then transformed into the weak form using the Galerkin method. The problem is solved using the finite element method by developing a three-node finite element with four degrees of freedom per node. The Newmark beta method is chosen for the time integration and the Gauss method for the spatial integration.

*Results:* The effects of several parameters were investigated, including the slenderness ratio, the material index, foundation stiffness, velocity and the frequency of the moving load. Good agreement was observed with the results obtained from the literature.

*Conclusion:* This study illustrates the importance of using a higher order theory in the case of short beams and clearly shows the change in the behavior of the FGM beam as a function of different parameters.

*Key words: higher-order shear deformation theory, functionally graded material, finite element method, moving load, Newmark beta method.*

## Introduction

Due to their importance, functionally graded materials (FGMs) have attracted the attention of many researchers around the world (Reddy, 2007; Menaa et al, 2012; Zemri et al, 2015; Berrabah & Boudierba, 2023). These new materials were initially created with the aim of using them as thermal barriers in high-temperature environments (Fuchiyama & Noda, 1995; Praveen & Reddy, 1998). Today, they are used in a wide range of engineering fields, including aerospace, nuclear energy, biology, electromagnetism, optics, energy and other fields through the ingenious combination of two or more materials such as metals, ceramics, and plastics (Saleh et al, 2020).

Literature related to this field is significant, including studies of bending, buckling, and free vibration (Dey et al, 2019). These studies have utilized various resolution methods, especially numerical and analytical techniques. Each of these two main methods has its advantages and disadvantages. The finite element method is one of the most widely used numerical methods for structural analysis because it offers both ease of programming and adaptability. One program can be used to solve a variety of problems with minimal changes, making it a highly efficient and flexible tool.

Extensive research has been conducted on the dynamic behavior of the FGM structures. Yang et al. (2008) conducted an analytical investigation on the vibrational behavior of Euler-Bernoulli beams with open edge cracks and exponential through-thickness variation in material properties. They considered the effects of axial compressive force and concentrated transverse load, and obtaining analytical solutions for natural frequencies and dynamic deflections of different boundary conditions beam types with exponential through-thickness variation in material properties. Şimşek & Kocatürk (2009) investigated the free vibration and dynamic behavior of a simply supported functionally graded beam under a concentrated moving harmonic load. Lagrange's equations, Euler-Bernoulli beam theory, and polynomial trial functions are employed to derive the equations of motion. Hasheminejad & Rafsanjani (2009) presented a precise three-dimensional analysis of the steady-state dynamic response of an arbitrarily thick, isotropic, and functionally graded plate strip under a transverse moving line load. Utilizing the Fourier transformation and a laminate model, Khalili et al. (2010) introduced a mixed method for analyzing the dynamic behavior of functionally graded



beams under moving loads. Utilizing Euler–Bernoulli beam theory and Lagrange equations, the Rayleigh–Ritz method discretizes spatial derivatives, while a step-by-step differential quadrature method (DQM) handles temporal derivatives. The proposed method demonstrated efficiency and reliability, providing improved accuracy compared to single-step methods like Newmark and Wilson. Şimşek (2010) investigated vibration of a functionally graded simply-supported beam, influenced by a moving mass using Euler–Bernoulli, Timoshenko, and third-order shear deformation beam theories. Yan et al. (2011) explored the dynamic response of functionally graded beams with an open-edge crack on an elastic foundation, subjected to a transverse load moving at a constant speed. Yan & Yang (2011) studied the forced flexural vibration of functionally graded beams with open-edge cracks under axial compressive force and moving transverse load, where the cracked section was modeled as a rotational spring and the vibration responses were determined using the modal series expansion technique. Le et al. (2014) developed a finite element procedure for analyzing the vibration of multi-span functionally graded material (FGM) beams under a moving harmonic load. The finite element formulation incorporated the exact solution of the FGM Timoshenko beam segment's governing differential equations, considering the shift in the neutral axis position. Malekzadeh & Monajjemzadeh (2016) explored the dynamic response of functionally graded (FG) beams in a thermal environment under the influence of a moving load, employing the first-order shear deformation theory (FSDT). Initial thermal stresses are determined through the solution of thermoelastic equilibrium equations. A finite element method solution procedure is developed for FG beams with various loading and boundary conditions. Lin & Lee (2016) predicted the instability and vibration of a concentrated mass moving along a curved beam. While the existing literature commonly approximates the moving mass model using the moving load model, this paper introduces a semi-analytical method for the moving mass problem and compares it with the traditional model. Wang et al. (2017) introduced a novel N-node weak form quadrature beam element, based on the physical neutral surface. Explicit formulas for stiffness and mass matrices computation are provided. This element is applied to analyze the dynamic behavior of functionally graded material beams subjected to a moving point load. Gan et al. (2017) explored the effects of an intermediate elastic support on the vibration behavior of functionally graded Euler-Bernoulli beams that are subjected to a moving point load. To analyze the dynamic responses, a finite element model is utilized, while a thorough examination of the stiffness and position of the elastic support sheds light on their impact on the dynamic

characteristics of the functionally graded material beams. Barati & Zenkour (2018) examined the behavior of forced vibration in functionally graded nanobeams, which is dependent on their size. This behavior occurs under in-plane hygro-thermal loading and lateral dynamic loads. By utilizing a higher-order refined beam theory that does not incorporate shear correction factors, the nanobeam interacts with a foundation that follows the three-parameter Kerr model. Beskou & Muho (2018) have studied analytically and numerically the dynamic response of a simply supported elastic beam on a Winkler-type elastic foundation with viscous damping to a harmonically varying, moving point load. Parametric assessments include the effects of foundation stiffness, damping, beam damping, and load acceleration, providing practical insights for various scenarios. Barati et al. (2019) explored the forced vibrations of nanobeams under the nonlocal strain gradient theory on a viscoelastic substrate subjected to moving loads. The nanobeam experiences varied hygro-thermal environments. Dynamic deflections were obtained using Galerkin and inverse Laplace transform methods. The influence of nonlocal parameter, strain gradient, moving load, temperature, moisture, and viscoelastic foundation on forced vibration behavior were discussed. Esen (2019) studied an improved Finite Element Method for analyzing transverse vibrations in Timoshenko beams made of functionally graded materials on a two-parameter foundation, under the influence of a variable-velocity moving mass. The investigation thoroughly explores the effects of inertia, foundation parameters, and material constituents, revealing significant changes in dynamic behavior shaped by frequency variations in the system. El Khouddar et al. (2024) analyzed gradient materials with piezoelectric actuators using the Euler–Bernoulli beam theory and the nonlinear Von-Karman deformation field. Analytical predictions for nonlinear free and forced vibrations of a beam on an elastic foundation were validated against the existing literature. Li et al. (2021) proposed an efficient method for accurate free vibration analysis of functionally graded beams with variable cross-sections on Pasternak elastic foundations. Utilizing the separate variable method and the Laplace transform, they provided general expressions for displacements and stresses, validated through various examples, offering a precise alternative for ultra-high precision requirements in mechanical systems. Esen et al. (2023) investigated the dynamic responses of Timoshenko beams with symmetric and sigmoid functionally graded gradations, resting on an elastic foundation and subjected to a moving mass. Using the Hamilton principle, system equations are derived and solved with a finite element method. Parametric studies explore influences of gradation type, index, elastic

foundation stiffness, inertia, and variable velocity of the moving mass. Javidi et al. (2023) presented an analytical study using the Optimal Homotopy Analysis Method and enriched multiple scales to investigate the dynamics of a beam with a moving mass and resting on a viscoelastic foundation. The authors considered a fifth-order nonlinear term to account for the bending vibration of the flexible beam and use the Galerkin method to form the corresponding ordinary differential equation. He et al. (2023) investigated the vibration of a cylindrical beam made of functionally graded materials under thermal conditions, validating the theoretical model against the finite element analysis. The displacement function was built using Carrera unified formulation, Taylor polynomials, and the improved Fourier series method. Guo et al. (2022) presented the dynamic analysis of exponentially functionally graded material micro plates with porosities. Utilizing the general third-order shear deformation theory and a modified couple stress theory, the research investigated the forced vibration response to accelerating moving loads. Safaei et al. (2024) investigated the out-of-plane free vibrational behaviors and responses to moving loads of sandwich-curved beams with graphene platelets reinforced composite face sheets and porous core (GPLRC-FS-PC). By employing the first-order shear deformation theory, the differential quadrature method, and Newmark's method, this study investigates the impacts of GPLs on the fundamental frequency and displacement amplitudes. It specifically accentuates the dependencies on distribution patterns as well as the ratio between the face sheet and the core thickness.

From this literature review, it is noted that a higher-order shear theory is rarely used to study the dynamic behavior of FGM beams under the effect of moving loads. In this context, the objective of this work is to present a three-node finite element model to study the dynamic behavior of an FGM beam under the effect of a harmonic moving load and on an elastic foundation, using a higher-order shear theory. Hamilton's principle is used to find the differential equations governing the behavior of the beam. Galerkin's method is used to transform the strong formulation into a weak one. Spacial integration is then performed using the Gauss method, and the Newmark beta method is used for time integration.

## Mathematical modeling

### *Properties of functionally graded materials*

This study examines a beam with dimensions of length ( $L$ ), thickness ( $h$ ), and width ( $b$ ) within the conventional Cartesian coordinate system ( $x$ ,

$y, z$ ), as illustrated in Figure 1. Herein, the longitudinal direction is denoted by  $x$ , and the vertical transverse direction is represented by  $z$ .

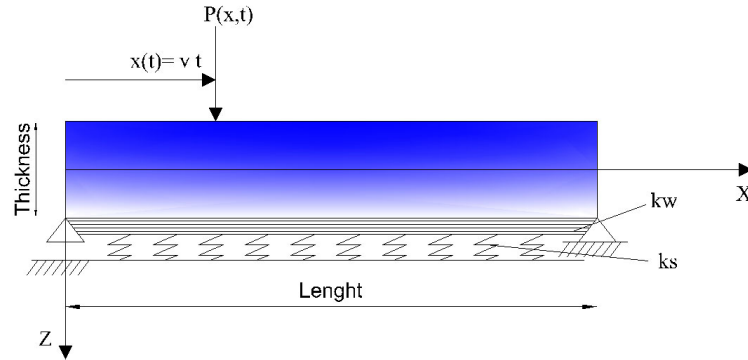


Figure 1 – FGM beam on a two-parameter linear elastic foundation subjected to a moving load

The material properties of the beam are assumed to be varied in the direction of thickness, in accordance with a polynomial function. These properties of each point in the beam can be written as a function of the volume fractions of each material constituting the beam under the following law:

$$P(z) = P_c V_c + P_m V_m \quad (1)$$

The mechanical property ' $P$ ' can be Young's modulus or mass density. The volume fraction of each material is denoted by ' $V$ ', with the subscripts ' $c$ ' and ' $m$ ' representing ceramic and metal components, respectively. The relationship between the fractions of metal and ceramic is expressed in the following manner (Ebrahimi & Jafari, 2018):

$$V_c + V_m = 1 \Rightarrow V_m = 1 - V_c \quad (2)$$

with  $V_c = \left( \frac{z}{h} + \frac{1}{2} \right)^k$  and  $k$  is a material index.

The law governing the combination of Young's modulus and the mass density within a mixture can be expressed as follows:

$$\begin{aligned} E(z) &= (E_c - E_m) \cdot V_c + E_m \\ \rho(z) &= (\rho_c - \rho_m) \cdot V_c + \rho_m \end{aligned} \quad (3)$$

The beam is subjected to a moving load, denoted as  $F(x,t)$ . This moving load maintains a constant velocity  $v$  as it traverses the beam from the left to the right. This moving load has the following expression:

$$F(x,t) = F_0 \cdot \sin(\Omega \cdot t) \quad (4)$$

where  $\Omega$  is the frequency of excitation.

The position of the load as a function of time can be determined through the following relation:

$$x(t) = v \cdot t + x_0 \quad (5)$$

$x_0$  is initial position when  $t=0$ . We take  $x_0=0$

The higher-order shear deformation theory is employed to represent the displacement field. In this theory, shear is considered through a function that represents the distortion of the cross-sectional area. Additionally, this theory ensures the nullity of shear forces at both the upper and lower interfaces. This field takes the following form (Thai & Vo, 2012):

$$u_1(x,z,t) = u(x,t) - z \cdot \frac{\partial w(x,t)}{\partial x} - f(z) \cdot \phi(x,t) \quad (6)$$

$$u_2(x,z,t) = w(x,t)$$

where  $u$ ,  $w$  and  $\phi$  represent the axial displacement, the transverse displacement and the shear rotation of the cross-section. Due to the negligible transverse deformations, all points within the same cross section have identical displacements. Thus, the  $w$  component is independent of  $z$ .  $f(z)$  is the  $n^{th}$ -order shape function of the transverse shear strains given by (Xiang & Kang, 2013; Nguyen & Phung, 2023):

$$f(z) = \frac{z}{n} \left( \frac{2z}{h} \right)^{n-1} \text{ with } n=3, 5, 7 \dots$$

The elastic strain at a given point in time is written in the following way:

$$\begin{aligned} \varepsilon_x &= \frac{\partial u(x,t)}{\partial x} - z \cdot \frac{\partial^2 w(x,t)}{\partial x^2} - f(z) \cdot \frac{\partial \phi(x,t)}{\partial x} \\ \gamma_{xz} &= f'(z) \cdot \frac{\partial w(x,t)}{\partial x} \end{aligned} \quad (7)$$

Hamilton's principle asserts that the time integral of the variation in total energy is zero when the system is in equilibrium. This principle can be expressed as follows:

$$\int_{t_1}^{t_2} (\delta U + \delta U_f - \delta V - \delta K) dt = 0 \quad (8)$$

$U$ ,  $U_f$ ,  $V$  and  $K$  denote the elastic deformation energy, the elastic foundation strain energy, the work of external forces, and the kinetic energy, respectively.

The elastic strain energy depends on the normal and tangential stresses and the corresponding strains. This association can be expressed as follows:

$$\delta U = \int (\sigma_x \delta \varepsilon_x + \tau_{xz} \delta \gamma_{xz}) dV = \int_0^L \left( N \frac{\partial \delta u}{\partial x} - M_b \frac{\partial^2 \delta w}{\partial x^2} + M_s \frac{\partial \delta \phi}{\partial x} + Q \delta \phi \right) dx \quad (9)$$

$N$ ,  $M_b$ ,  $M_s$  and  $Q$  represent the internal forces which are defined by the following expressions:

$$\begin{aligned} \{N, M_b, M_s\} &= \int \sigma_x \{1, z, f(z)\} dz \\ Q &= \int G(z) f'(z) dz \end{aligned} \quad (10)$$

The determination of the strain energy in an elastic foundation is carried out using the subsequent expression:

$$\delta U_f = \int_0^L \left( k_w \delta w - k_s \frac{\partial^2 \delta w}{\partial x^2} \right) dx \quad (11)$$

where  $k_w$  and  $k_s$  are the Winkler elastic foundation and the shear foundation modulus.

The work of the external forces can be written as follows:

$$\delta V = \int_0^L (q \delta w) dx + \int_0^L (F(x, t) \cdot \delta x(t) \cdot \delta w) dx \quad (12)$$

with  $q$  being the load distributed over the length of the beam.

The variation in the kinetic energy of the beam is as follows:

$$\delta K = \int_0^L \int_{-h/2}^{h/2} \rho(z) \left( \dot{u} \delta \dot{u} + \dot{w} \delta \dot{w} \right) dx \quad (13)$$



$$= \int_0^L \left( -I_0 \ddot{u} \delta u - I_1 \frac{\partial \ddot{u}}{\partial x} \delta w - K_1 \ddot{u} \delta \phi + I_1 \frac{\partial \ddot{w}}{\partial x} \delta u + I_2 \frac{\partial^2 \ddot{w}}{\partial x^2} \delta w + K_2 \frac{\partial \ddot{w}}{\partial x} \delta \phi - K_1 \ddot{\phi} \delta u - K_2 \frac{\partial \ddot{\phi}}{\partial x} \delta w - J \ddot{\phi} \delta \phi - I_0 \ddot{w} \delta w \right) dx$$

where  $\{I_0, I_1, I_2, K_1, K_2, J\} = \int \rho(z) \{1, z, z^2, f(z), zf(z), f(z)^2\} dz$

By substituting equations (9), (11), (12), and (13) in equation (8), one obtains the following system of differential equations:

$$\begin{aligned} \delta u : -\frac{\partial N}{\partial x} &= -I_0 \ddot{u} + I_1 \frac{\partial \ddot{w}}{\partial x} - K_1 \ddot{\phi} \\ \delta w : -\frac{\partial^2 M_b}{\partial x^2} - kw + \frac{\partial^2 k_s}{\partial x^2} &= -I_1 \frac{\partial \ddot{u}}{\partial x} + I_2 \frac{\partial^2 \ddot{w}}{\partial x^2} - K_2 \frac{\partial \ddot{\phi}}{\partial x} - I_0 \ddot{w} \\ &+ q + F(x, t) \end{aligned} \quad (14)$$

$$\delta \phi : -\frac{\partial M_s}{\partial x} + Q = -K_1 \ddot{u} + K_2 \frac{\partial \ddot{w}}{\partial x} - J \ddot{\phi}$$

The relationship between stresses and strains can be written using Hooke's law:

$$\begin{aligned} \sigma_x &= E(z) \varepsilon_x \\ \tau_{xz} &= G(z) \gamma_{xz} \end{aligned} \quad (15)$$

By integrating the given expression (10) and the corresponding equations (15), one can formulate the internal forces in the following manner:

$$\begin{aligned} N &= A \frac{\partial u}{\partial x} - B \frac{\partial^2 w}{\partial x^2} + C \frac{\partial \phi}{\partial x} \\ M_b &= B \frac{\partial u}{\partial x} - B_s \frac{\partial^2 w}{\partial x^2} + D_s \frac{\partial \phi}{\partial x} \\ M_s &= C \frac{\partial u}{\partial x} - D_s \frac{\partial^2 w}{\partial x^2} + H_s \frac{\partial \phi}{\partial x} \\ Q &= H_{s2} \phi \end{aligned} \quad (16)$$

with:  $\{A, B, C, B_s, D_s, H_s\} = \int E(z) \{1, z, f(z), z^2, zf(z), f(z)^2\} dz$  and

$$H_{s2} = \int G(z) g(z)^2 dz$$

By replacing expressions (16) in the system of equations (14), the differential equations in terms of displacement under moving force of FGM beams with the presence of a foundation are obtained as follows:

$$-A \frac{\partial^2 u}{\partial x^2} + B \cdot \frac{\partial^3 w}{\partial x^3} - C \cdot \frac{\partial^2 \phi}{\partial x^2} = -I_0 \ddot{u} + I_1 \frac{\partial \ddot{w}}{\partial x} - K_1 \phi \quad (17a)$$

$$\begin{aligned} & -B \frac{\partial^3 u}{\partial x^3} + B_s \cdot \frac{\partial^4 w}{\partial x^4} - D_s \cdot \frac{\partial^3 \phi}{\partial x^3} - k_w + \frac{\partial^2 k_s}{\partial x^2} \\ & = -I_1 \frac{\partial \ddot{u}}{\partial x} + I_2 \frac{\partial^2 \ddot{w}}{\partial x^2} - K_2 \frac{\partial \ddot{\phi}}{\partial x} - I_0 \ddot{w} + q + F(x, t) \end{aligned} \quad (17b)$$

$$C \frac{\partial^2 u}{\partial x^2} - D_s \cdot \frac{\partial^3 w}{\partial x^3} - H_s \cdot \frac{\partial^2 \phi}{\partial x^2} + H_{s2} = -K_1 \ddot{u} + K_2 \frac{\partial \ddot{w}}{\partial x} - J \ddot{\phi} \quad (17c)$$

### ***Galerkin finite element formulation***

There are several techniques for discretizing the system of differential equations, among which the Galerkin finite element method is a widely used and effective technique (Phadikar & Pradhan, 2010). By using this method, the following weak form is obtained:

$$\begin{aligned} & \int_{x_1^e}^{x_2^e} \left( -A \frac{\partial \psi}{\partial x} \frac{\partial u}{\partial x} + B \cdot \frac{\partial \psi}{\partial x} \frac{\partial^2 w}{\partial x^2} - C \cdot \frac{\partial \psi}{\partial x} \frac{\partial \phi}{\partial x} \right) dx \\ & = \int_{x_1^e}^{x_2^e} \psi \left( -I_0 \ddot{u} + I_1 \frac{\partial \ddot{w}}{\partial x} - K_1 \phi \right) dx \end{aligned} \quad (18a)$$

$$\begin{aligned} & \int_{x_1^e}^{x_2^e} \left( -B \frac{\partial^2 \psi}{\partial x^2} \frac{\partial u}{\partial x} + B_s \cdot \frac{\partial^2 \psi}{\partial x^2} \frac{\partial^2 w}{\partial x^2} - D_s \cdot \frac{\partial^2 \psi}{\partial x^2} \frac{\partial \phi}{\partial x} - \psi(kw) \right) dx \\ & = - \int_{x_1^e}^{x_2^e} \left( I_1 \frac{\partial \psi}{\partial x} \ddot{u} + I_2 \frac{\partial \psi}{\partial x} \frac{\partial \ddot{w}}{\partial x} - K_2 \frac{\partial \psi}{\partial x} \ddot{\phi} - I_0 \psi \ddot{w} - \psi(q + F(x, t)) \right) dx \end{aligned} \quad (18b)$$

$$\int_{x_1^e}^{x_2^e} \left( C \frac{\partial \psi}{\partial x} \frac{\partial u}{\partial x} - D_s \cdot \frac{\partial \psi}{\partial x} \frac{\partial^2 w}{\partial x^2} - H_s \cdot \frac{\partial \psi}{\partial x} \frac{\partial \phi}{\partial x} + H_{s2} \psi \phi \right) dx$$

$$= \int_{x_1^e}^{x_2^e} \left( -K_1 \ddot{u} + K_2 \frac{\partial \ddot{w}}{\partial x} - J \ddot{\phi} \right) dx \quad (18c)$$

with  $\psi$  being the weight function.

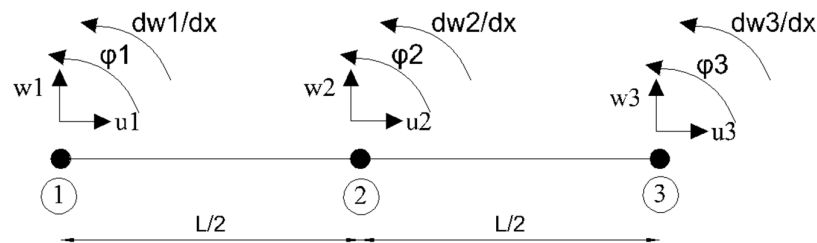


Figure 2 – Finite beam element with three nodes and three degrees of freedom per node

In order to construct the finite element beam employed in this study, we will consider a Hermitian element with three nodes (Figure 2). The displacements  $u$ ,  $w$ , and  $\phi$  are expressed in the subsequent manner:

$$u = [N_1 \quad N_2 \quad N_3] \begin{Bmatrix} u_1 \\ u_2 \\ u_3 \end{Bmatrix} \quad (19a)$$

$$\phi = [N_1 \quad N_2 \quad N_3] \begin{Bmatrix} \phi_1 \\ \phi_2 \\ \phi_3 \end{Bmatrix} \quad (19b)$$

$$w = [N_{w1} \quad N_{w2} \quad N_{w3} \quad N_{w4} \quad N_{w5} \quad N_{w6}] \begin{Bmatrix} w_1 \\ \theta_1 \\ w_2 \\ \theta_2 \\ w_3 \\ \theta_3 \end{Bmatrix} \quad (19c)$$

$N_i$  and  $N_{w_i}$  are the polynomial shape functions related to nodes, given by the following expressions:

$$N_1 = 1 - \frac{3x}{L} + \frac{2x^2}{L^2} \quad (20a)$$

$$N_2 = \frac{4x}{L} - \frac{4x^2}{L^2} \quad (20b)$$

$$N_3 = -\frac{x}{L} + \frac{2x^2}{L^2} \quad (20c)$$

$$N_{w1} = 1 - \frac{23x^2}{L^2} + \frac{66x^3}{L^3} - \frac{68x^4}{L^4} + \frac{24x^5}{L^5} \quad (20d)$$

$$N_{w2} = x - \frac{6x^2}{L^2} + \frac{13x^3}{L^3} - \frac{12x^4}{L^4} + \frac{4x^5}{L^5} \quad (20e)$$

$$N_{w3} = \frac{16x^2}{L^2} - \frac{32x^3}{L^3} + \frac{16x^4}{L^4} \quad (20f)$$

$$N_{w4} = -\frac{8x^2}{L^2} + \frac{32x^3}{L^3} - \frac{40x^4}{L^4} + \frac{16x^5}{L^5} \quad (20g)$$

$$N_{w5} = \frac{7x^2}{L^2} - \frac{34x^3}{L^3} + \frac{52x^4}{L^4} - \frac{24x^5}{L^5} \quad (20h)$$

$$N_{w6} = -\frac{x^2}{L^2} + \frac{5x^3}{L^3} - \frac{8x^4}{L^4} + \frac{4x^5}{L^5} \quad (20i)$$

and  $\theta = \frac{\partial w}{\partial x}$ .

Using the shape functions in the weak form and integrating along the length of element, we obtain the following elementary equation:

$$\left( [K^{elem}] + [K_f^{elem}] \right) \{U^{elem}\} + [M^{elem}] \left\{ \ddot{U}^{elem} \right\} = \{F^{elem}\} \quad (21)$$

$K^{elem}$ ,  $K_f^{elem}$ ,  $U^{elem}$ ,  $M^{elem}$  and  $F^{elem}$  are the elemental beam's stiffness matrix, the foundation stiffness matrix, the displacement vector, the mass matrix, and the vector of external forces. The elemental equations can be assembled to form global equations and one can solve the simultaneous

algebraic equations. Three separates analyses have been used for solving this problem. Table 1 shows these three systems of equations.

Table 1 – Three systems of equations to be analysed

$([K] + [K_f])\{U\} = \{F\}$	for solving the static problem by applying static concentrated force $P_0$ at the mid span, in the first case, and a uniform distributed load, in the second case
$([K] + [K_f])\{U\} + [M]\{\ddot{U}\} = 0$	for solving the free vibration problem and obtaining the natural frequencies
$([K] + [K_f])\{U\} + [M]\{\ddot{U}\} = \{F\}$	for solving the forced vibration problem by applying the moving laod $P(x,t)$ . The Newmark $\beta$ method is used for integrating in time the system of equations.

For the case of forced vibration, the Newmak  $\beta$  method is used to integrate the system of equations. Newmark's  $\beta$  method is considered to be a special type of finite difference techniques commonly used by engineers and researchers to solve second-order differential equations with multiple degrees of freedom. The authors present here a summary of the methodology introduced by Newmark (Chopra, 2014; Yang et al, 2004).

The equations of motion of the structure at time  $t+\Delta t$  are as follows:

$$([K] + [K_f])\{U\}_{t+\Delta t} + [C]\{\dot{U}\}_{t+\Delta t} + [M]\{\ddot{U}\}_{t+\Delta t} = \{F\}_{t+\Delta t} \quad (22)$$

where  $\Delta t$  is a small time increment, and  $[C]$  is the damping matrix wich is neglected in this work.

Newmark's method is characterized by its one-step approach, requiring only information from the structure at time  $t$  for resolution. The method uses two fundamental equations proposed by Newmark to determine the displacements and velocities of the structure at time  $t+\Delta t$ :

$$\begin{aligned} \{U\}_{t+\Delta t} &= \{U\}_t + \{\dot{U}\}_t \Delta t + \left[ \left( \frac{1}{2} - \beta \right) \{\ddot{U}\}_t + \beta \{\ddot{U}\}_{t+\Delta t} \right] (\Delta t)^2 \\ \{\dot{U}\}_{t+\Delta t} &= \{\dot{U}\}_t + \left[ (1 - \gamma) \{\ddot{U}\}_t + \gamma \{\ddot{U}\}_{t+\Delta t} \right] \Delta t \end{aligned} \quad (23)$$

The method has been shown to be unconditionally stable under the conditions where  $\gamma \geq 1/2$  and  $\beta \geq 1/4(1/2 + \gamma)^2$ . Throughout this paper, the combination of  $\gamma = 1/2$  and  $\beta = 1/4$  will be chosen.

The accelerations and velocities of the structure at time  $t+\Delta t$  can be determined from equation (23):

$$\begin{aligned} \left\{ \ddot{U} \right\}_{t+\Delta t} &= a_0 \left( \left\{ U \right\}_{t+\Delta t} - \left\{ U \right\}_t \right) - a_2 \left\{ \dot{U} \right\}_t - a_3 \left\{ \ddot{U} \right\}_t \\ \left\{ \dot{U} \right\}_{t+\Delta t} &= \left\{ \dot{U} \right\}_t + a_6 \left\{ \ddot{U} \right\}_t + a_7 \left\{ \ddot{U} \right\}_{t+\Delta t} \end{aligned} \quad (24)$$

The coefficients  $a_0$  to  $a_7$  are provided as follows:

$$\begin{aligned} a_0 &= \frac{1}{\beta \Delta t^2}, \quad a_1 = \frac{\gamma}{\beta \Delta t}, \quad a_2 = \frac{1}{\beta \Delta t}, \quad a_3 = \frac{1}{2\beta} - 1, \quad a_4 = \frac{\gamma}{\beta} - 1, \\ a_5 &= \frac{\Delta t}{2} \left( \frac{\gamma}{\beta} - 2 \right), \quad a_6 = \Delta t (1 - \gamma), \quad a_7 = \gamma \Delta t \end{aligned} \quad (25)$$

By substituting the preceding expression (24) into equation (22), the equivalent stiffness equations are obtained:

$$[K_{eff}] \{U\}_{t+\Delta t} = \{F_{eff}\}_{t+\Delta t} \quad (26)$$

where the effective stiffness matrix  $[K_{eff}]$  and the effective load vector  $\{P_{eff}\}_{t+\Delta t}$  are defined as follows:

$$\begin{aligned} [K_{eff}] &= a_0 [M] + a_1 [C] + ([K] + [K_f]) \\ \{P_{eff}\}_{t+\Delta t} &= \{P\}_{t+\Delta t} \\ &+ [M] \left( a_0 \left\{ \dot{U} \right\}_t + a_2 \left\{ \dot{U} \right\}_t + a_3 \left\{ \ddot{U} \right\}_t \right) + [C] \left( a_1 \left\{ \dot{U} \right\}_t + a_4 \left\{ \dot{U} \right\}_t + a_5 \left\{ \ddot{U} \right\}_t \right) \end{aligned} \quad (27)$$

Based on equation (26), the structural displacements  $\{U\}$  at time  $t+\Delta t$  can be calculated as follows:

$$\{U\}_{t+\Delta t} = [K_{eff}]^{-1} \{F_{eff}\}_{t+\Delta t} \quad (28)$$

The three sets of equations for static, free, and forced vibration problems were solved using a MATLAB algorithm specifically developed for this purpose.

## Numerical results

The numerical results examine the static, free and forced vibrations of the simply supported (SS) FG beam subjected to moving harmonic loads.

### Validation study

The results obtained from the formulation presented in this article are confirmed through validation against other studies. To this end, we compare the static responses and free vibration natural frequencies with the results reported in the references. The characteristics adopted are as follows (Şimşek & Al-shujairi, 2017):

- Steel:  $E_m=70$  GPa,  $\rho_m=2702$  kg/m<sup>3</sup>,  $\nu_m=0.3$ .
- Alumina:  $E_c=380$  GPa,  $\rho_c=3960$  kg/m<sup>3</sup>,  $\nu_c=0.3$ .

Table 2 shows the maximum transverse deflection of an FGM beam simply supported under a uniformly distributed load compared with the results found in the literature (Şimşek & Al-shujairi, 2017).

Table 2 – Non-dimensional deflection of the mid-span of FG beam under uniform load

L/h		k		
		0	1	10
5	CBT	2.8783	5.7746	9.6072
	TBT	3.1657	6.2599	10.7194
	Presente	3.0107	5.9983	10.0200
20	CBT	2.8783	5.7746	9.6072
	TBT	2.8962	5.8049	9.6767
	Presente	2.8866	5.7886	9.6330

The following dimensionless quantities are used:

$$\bar{\omega} = \frac{\omega L^2}{h} \sqrt{\frac{\rho_m}{E_m}}$$

$$\bar{w} = 100 \frac{E_m h^3}{q L^4} w(L/2) \text{ for a Simply-Simply beam (SS) and a Clamped-}$$

Clamped (CC)

$$\bar{w} = 100 \frac{E_m h^3}{q L^4} w(L) \text{ for a Clamped-Free beam (CF)}$$

$$K_w = \frac{k_w \cdot L^4}{E_m I}, \quad K_s = \frac{k_s \cdot L^2}{E_m I}.$$

Firstly, it is observed that the present work's values of dimensional static deflection agree well with those of the references. It is evident that the deflection of FG beam increases with increasing the material index  $k$ . This trend is explained by the fact that when the gradient index increases, the modulus of elasticity and the stiffness of the beam decrease and the beam becomes more flexible.

Table 3 – First three non-dimensional frequencies of the FG SS beam for the slenderness ratios 5 and 20 and the gradient index  $k$  (0, 1, and 10)

			<b>k</b>		
L/h	mode		0	1	10
5	1	CBT	5.3953	4.1484	3.4921
		TBT	5.1527	3.9904	3.2816
		Presente	5.1910	4.0151	3.3587
	2	CBT	20.6187	15.7982	13.2376
		TBT	17.8812	14.0100	11.0240
		Presente	15.0990	14.6846	11.9147
	3	CBT	43.3483	33.0278	27.4752
		TBT	34.2097	27.0979	20.5561
		Presente	33.0444	27.0358	21.7556
20	1	CBT	5.4777	4.2163	3.5547
		TBT	5.4603	4.2051	3.5390
		Presente	5.4640	4.2075	3.5457
	2	CBT	21.8438	16.8100	14.1676
		TBT	21.5732	16.6344	13.9263
		Presente	21.6279	16.6685	14.0248
	3	CBT	48.8999	37.6173	31.6883
		TBT	47.5930	36.7679	30.5369
		Presente	47.8323	36.8329	30.8015

In the second part of the validation study, the vibratory characteristics of the studied FGM beam are analyzed. Table 3 shows the first three natural frequencies of vibration of an FGM beam for different values of  $k$



and for two values of the  $L/h$  ratio, compared with the results found in the references (Şimşek & Al-Shujairi, 2017). Table 4 shows the non-dimensional frequencies of the FG beam for tow slenderness ratios (10 and 100) and several values of the index  $k$  (0, 1 and 10) compared with the results found in the references (Zemri et al, 2015).

Table 4 – Non-dimensional frequencies of the FG SS beam for the slenderness ratios 10 and 100 and the gradient index  $k$  (0, 1, and 10)

		$k$		
$L/h$		0	1	10
10	TBT	5.3383	2.4194	1.5799
	(Zemri et al, 2015)	5.3383	2.4194	1.579
	Presente	5.3287	2.418	1.5771
100	TBT	5.2096	2.3679	1.5453
	(Zemri et al, 2015)	5.2096	36794	1.5454
	Presente	5.2091	2.3674	1.5452

Table 5 – Non-dimensional frequencies of the FG beam for the slenderness ratios 5 and 20 and different cases of boundary conditions (SS, CC, and CF)

		$k$			
$L/h$	Boundary conditions		0	1	10
5	SS	TBT	5.1524	3.9708	3.2960
		Presente	5.1910	4.0151	3.3587
	CC	TBT	9.9975	7.8997	6.3147
		Presente	10.3200	8.2828	6.8150
	CF	TBT	1.8944	1.4627	1.2236
		Presente	1.9034	1.4721	1.2370
20	SS	TBT	5.4603	4.2036	3.5403
		Presente	5.4640	4.2075	3.5457
	CC	TBT	12.2201	9.4292	7.9101
		Presente	12.2621	9.4716	7.9701
	CF	TBT	1.9495	1.5010	1.2649
		Presente	1.9502	1.5017	1.2659

The results obtained in the present study were compared to those calculated using the Timoshenko beam theory, TBT. Notably, a good agreement was observed with the results in the references. The provided table clearly indicates that the fundamental non-dimensional frequency decreases as the power law index increases, emphasizing the influence of this index on the beam's behavior.

In Table 5, the non-dimensional frequencies of the FG beam are compared with the results found by Şimşek & Al-shujairi (2017) for different cases of boundary conditions (SS, CC, and CF). An excellent agreement is observed.

### Convergence study

Firstly, the convergence of the results of the model developed in this study must be studied. For this purpose, an isotropic beam is taken with the following characteristics:  $E=380$  MPa,  $L=10$ m  $b=1$ m,  $F_0=100$ KN,  $\Omega=0$ . Two values of the  $L/h$  ratio are considered, namely  $L/h=5$  and  $L/h=20$  and with two speeds  $v=20$ Km/h and  $v=100$ Km/h.

The results of the convergence study of the static and dynamic deflection and the free vibration frequency of the isotropic beam under the effect of a moving concentrated load, as a function of the number of finite elements, are shown in Figures 3, 4, 5 and 6.

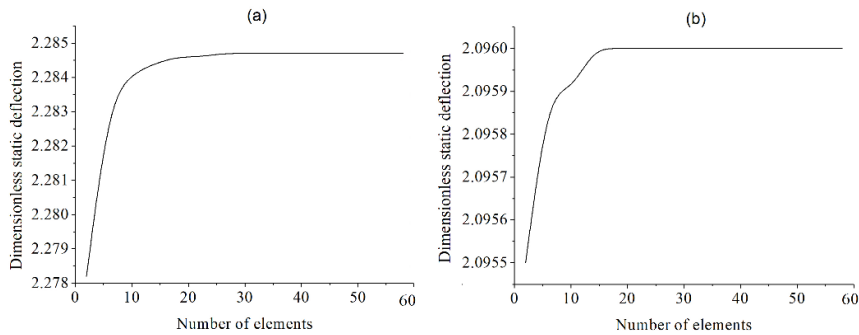


Figure 3 – Study of convergence of the dimensionless static deflection for: a)  $L/h=5$  and b)  $L/h=20$

From these figures, it can be seen that the deflection converges rapidly (by using 5, 10, or 15 elements) for the two cases of the  $L/h$  ratio and two cases of speed.

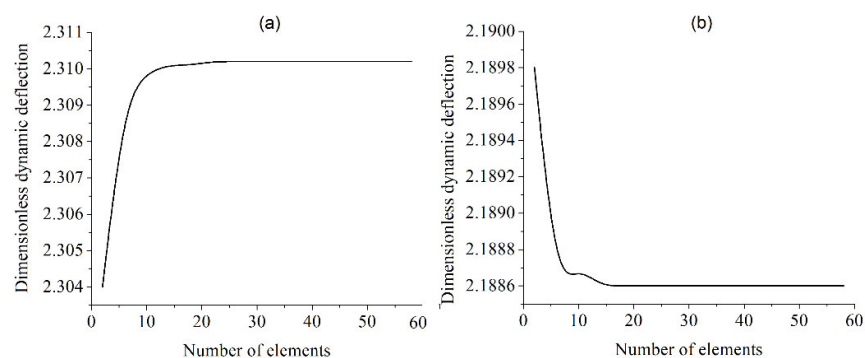


Figure 4 – Study of convergence of the dimensionless dynamic deflection with  $v=20\text{m/s}$  for: a)  $L/h=5$  and b)  $L/h=20$

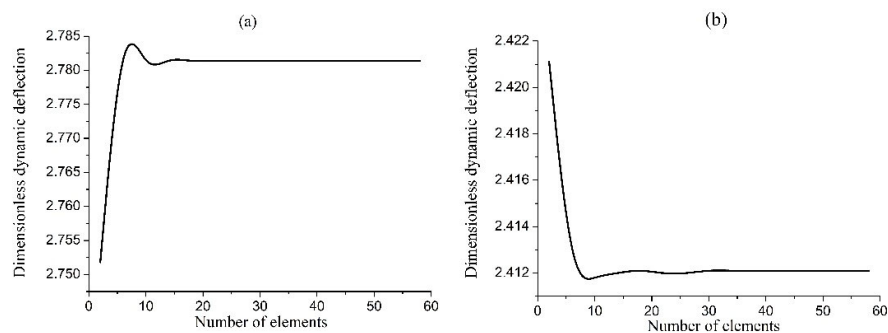


Figure 5 – Study of convergence of the dimensionless dynamic deflection with  $v=100\text{m/s}$  for: a)  $L/h=5$  and b)  $L/h=20$

For the natural frequency (Figure 7), it can be seen that fewer than 10 elements are sufficient for the frequency value to converge. In our work, 30 elements are used to discretize the FGM beam for all the cases studied.

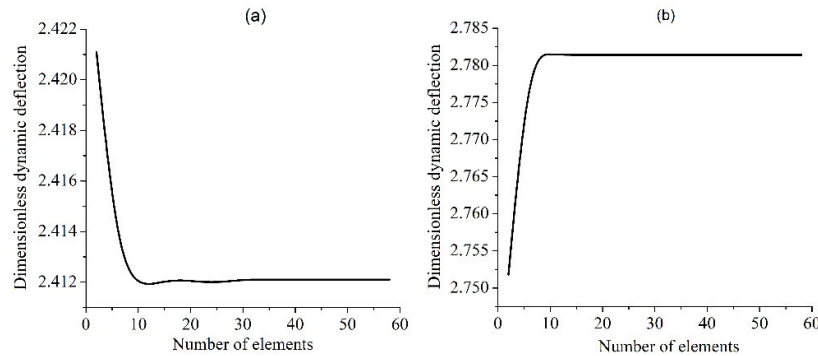


Figure 6 – Study of convergence of the dimensionless dynamic deflection for: a)  $L/h=5$  and b)  $L/h=20$

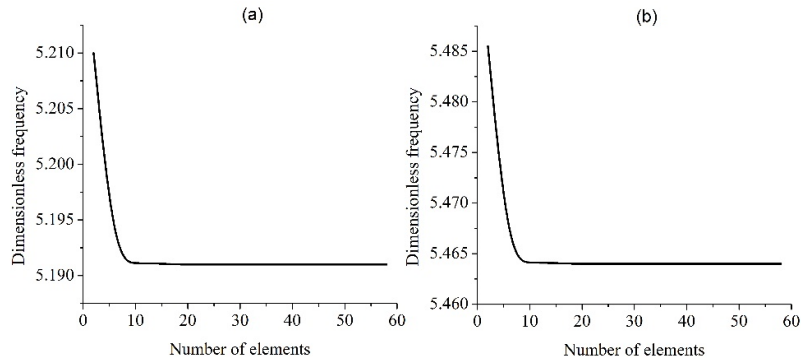


Figure 7 – Study of convergence of the dimensionless frequency for: a)  $L/h=5$  and b)  $L/h=20$

### Forced vibration

This section studies the forced vibration of the FG beam under the effect of a moving load with a constant velocity. It considers a beam with the following characteristics:  $L=20\text{m}$ ,  $h=0.9\text{m}$ ,  $b=0.4\text{m}$ ,  $E_f=210\text{ MPa}$ ,  $\rho_f=8166\text{ kg/m}^3$ ,  $E_b=390\text{ MPa}$ ,  $\rho_b=3960\text{ kg/m}^3$  and the material index  $k=0$ .

The dynamic amplification factor is defined as the ratio between the maximum dynamic deflection at the mid-span and the maximum static deflection at the same section.

For the purpose of validation of our formulation, the dynamic amplification factor (DAF) obtained by our study is compared with the results of Ismail Esen's article (Esen, 2019) for various values of  $k$  and shown in Table 5. Each value of the DAF is related with its corresponding velocity of the moving load expressed in  $m/s$ . A good agreement is found between the results of this work and those found in the reference.

Table 6 – DAF and corresponding velocities of the FG beam for different values of  $k$

Source	Ceramic	$k=0.2$	$k=0.5$	$k=1$	$k=2$	Metal
Reference (Esen, 2019)	0.9326 (252 m/s)	1.0336 (222 m/s)	1.1435 (198 m/s)	1.269 (179 m/s)	1.3365 (164 m/s)	1.7316 (132 m/s)
Present	0.9371 (250 m/s)	1.0382 (218 m/s)	1.1488 (194 m/s)	1.2554 (174 m/s)	1.3433 (160)	1.7403 (127 m/s)

By increasing the value of  $k$  the dynamic amplification factor increases and the corresponding velocity decreases. This is due to the fact that the increase in  $k$  corresponds to an increase in Young's modulus, which means that the beam is more flexible and therefore a lower speed of the moving load is required to achieve the maximum displacement.

Table 6 shows the variation of the dimensionless fundamental frequency for different values of  $L/h$  and different values of  $K_w$  and  $K_s$  compared with the results found in Chen et al. (2004). There is also good agreement between the results obtained by the present model and those found in the literature.

For the subsequent figures, the following characteristics are considered:  $E_t=320.23 \times 10^9$  MPa;  $\rho_t=3750$  kg/m<sup>3</sup>;  $E_b=207.78 \times 10^9$  MPa;  $\rho_b=8166$  kg/m<sup>3</sup>.

Figure 8 shows the dynamic mid-span displacement of an isotropic beam as a function of time under the effect of a moving load of a constant value over time. The length  $L=5$ m, the width  $b=1$ m, and the slenderness ratio  $L/h=5$ . The values of this displacement are multiplied by  $10^4$  for greater visibility. Several values of the moving load speed are taken. It can be seen that the amplitude of the vibration increases proportionally with

the speed. The maximum difference between the amplitude obtained by the two speeds 5 m/s and 120 m/s is of the order of 14.77%.

Table 7 – Variation of the dimensionless fundamental frequency for different values of L/h and different values of Kw and Ks

Kw	Ks	L/h=120		L/h=15		L/h=5	
		Reference (Chen et al, 2004)	Present	Reference (Chen et al, 2004)	Present	Reference (Chen et al, 2004)	Present
0	0	3.1414	3.1414	3.1323	3.1318	3.0637	3.0567
	100	3.7359	3.7365	3.7278	3.7238	3.6665	3.6739
	250	4.2969	4.2974	4.2889	4.2810	4.2232	4.2329
100	0	3.7482	3.7942	3.7401	3.7861	3.6788	3.7339
	100	4.1436	4.1739	4.1356	3.8298	4.0720	4.1160
	250	4.5823	4.6000	4.5741	3.8923	4.5028	4.5428
10000	0	10.0240	10.2602	9.9958	10.2286	7.3408	7.2772
	100	10.0481	10.2825	10.0197	10.2558	7.3410	7.2772
	250	10.0839	10.3161	10.0552	10.2342	7.3412	7.2772

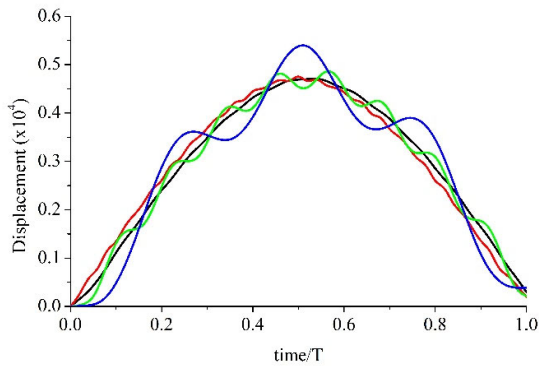


Figure 8 – Time history of the mid-span displacements of a simply supported isotropic beam: a) v=5 m/s, b) v=20 m/s, c) v= 50 m/s et d) v=120 m/s

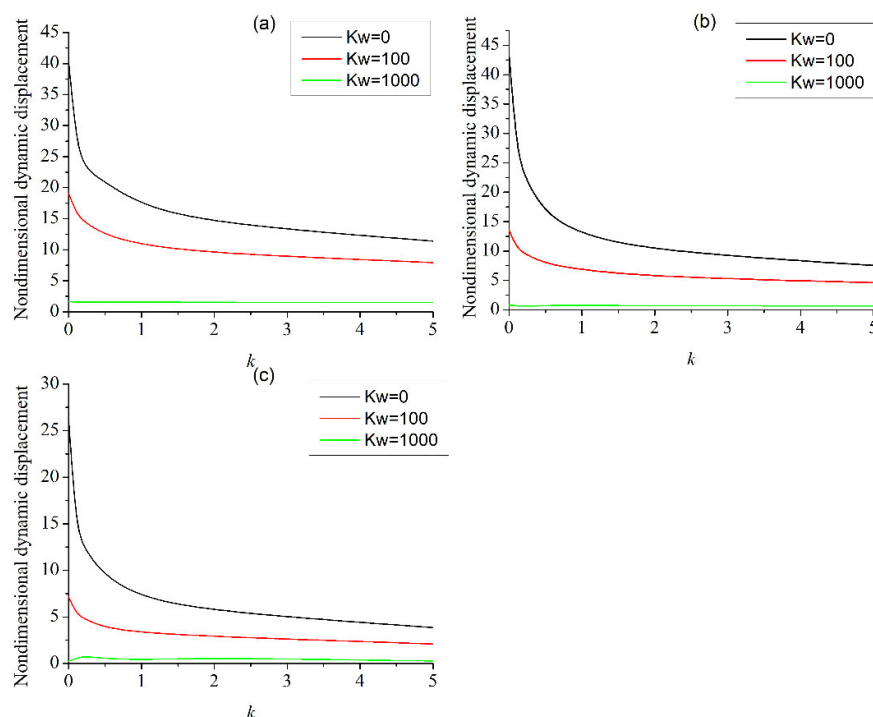


Figure 9 – Non-dimensional dynamic displacement of the mid-span section as a function of the index  $k$  for different values of  $K_w$  for: a)  $L/h=20$  b)  $L/h=10$  and c)  $L/h=5$

Figure 9 shows the maximum dimensional displacement at the mid-span of an FGM beam as a function of the index  $k$  for different values of the foundation stiffness  $K_w$  and three slenderness ratios  $L/h=5$ ,  $L/h=10$  and  $L/h=20$ . The transverse displacement values decrease as  $k$  increases. Increasing the value of  $k$  leads to an increase in Young's modulus, i.e., greater stiffness.

The presence of the elastic foundation leads to a decrease in beam displacements. The non-dimensional displacements are almost the same in the two cases of  $L/h=20$  and  $L/h=10$ . For the short beam ( $L/h=5$ ), there is a decrease in this value due to the main effect of the shear force in short beams.

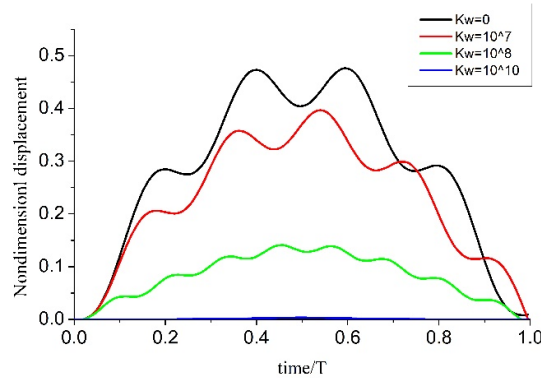


Figure 10 – Time history of the mid-span displacements of a simply supported FG beam for  $k=1$  and  $v=50\text{m/s}$

Figure 10 shows the effect of the elastic foundation on the forced vibration of an FGM beam ( $k=1$ ) subjected to a moving load with a speed of 50 m/s.  $T$  is the time taken for the moving load to traverse the beam from left to right. There is:  $T = \frac{L}{v}$ . It is clear that the amplitude of vibration decreases with increasing the elastic foundation coefficient  $K_w$ .

Figures 11, 12, 13, and 14 show the dynamic amplification factor of a simply supported FGM beam. This factor represents the ratio between the maximum dynamic displacement at mid-span and the static displacement at the mid-span, which is equal to  $\frac{P_0 L^3}{48 E_c I}$ . The following characteristics are taken:  $E_f=320.23 \times 10^9$  MPa,  $\rho_f=3750$  kg/m<sup>3</sup>,  $E_b=207.78 \times 10^9$  MPa,  $\rho_b=8166$  kg/m<sup>3</sup>,  $L=20\text{m}$ , and  $b=0.5\text{m}$ .

Figure 11 shows the variation of the dynamic amplification factor of an FGM beam as a function of the velocity of the moving load and the index  $k$ , with  $L/h=20$ : (a)  $K_w=0$  and  $K_s=0$  and (b)  $K_w=1000$  and  $K_s=100$ . The impact of velocity on the beam's response is evident in this figure. By increasing the speed, the DAF increases to reach its maximum and then decreases again. This factor reaches the same maximum value of 1.73 for all values of  $k$  but at different corresponding speeds: 260m/s for  $k=0$ , 230m/s for  $k=0.2$ , 180m/s for  $k=1$ , 170m/s for  $k=2$  and 140m/s for  $k=1000$ . Analyzing Figure 8(b), we can see that the presence of the elastic foundation results in a reduction of system flexibility, leading to a decrease in the normalized mid span deflection.



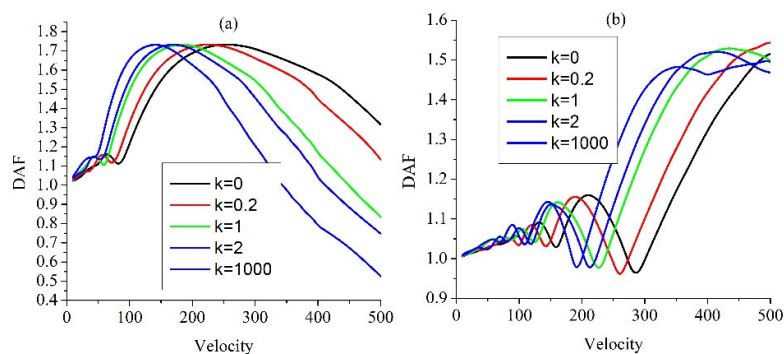


Figure 11 – Variation of the DAF as a function of velocity and the index  $k$ , for  $L/h=20$  (a)  $K_w=0$  et  $K_s=0$  (b)  $K_w=1000$  et  $K_s=100$

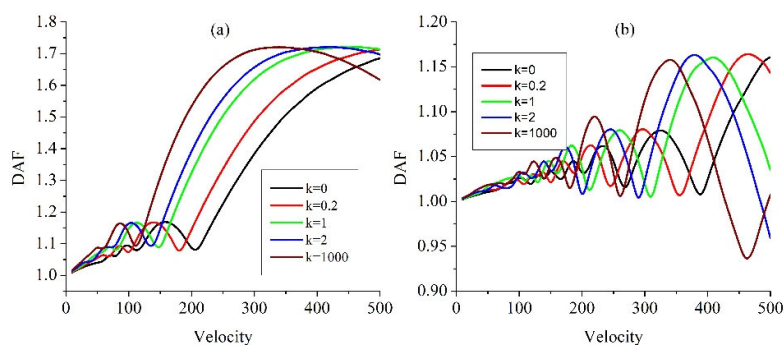


Figure 12 – Variation of the DAF as a function of velocity and the index  $k$  for  $L/h=8$  (a)  $K_w=0$  et  $K_s=0$  (b)  $K_w=1000$  et  $K_s=100$

Figure 12 shows the variation of the DAF as a function of speed and the index  $k$  for  $L/h=8$ . The same thing can be seen here as in the previous figure (Figure 12) but with higher values of corresponding velocities. These results reveal that the maximum dynamic magnification factors remain independent of the power-law exponent  $k$ .

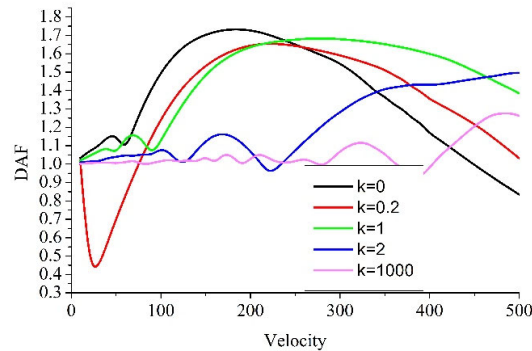


Figure 13 – Variation of the DAF as a function of  $K_w$  for  $k=1$  and  $L/h=20$

The variation of the DAF as a function of the speed of the moving load and for different values of  $K_w$  is shown in Figure 13. By increasing the value of the foundation stiffness, the DAF maximum value is reduced and reaches its maximum at higher values of speed. In the cases of  $K_w = 0$ , 10, and 100, the graphs show greater stability and reach higher maximum values compared to the case with  $K_w = 1000$  and 10000. The increase in the stiffness of the elastic foundation leads to an increase in the rigidity of the beam-foundation system and consequently to smaller values of transverse displacement of the beam.

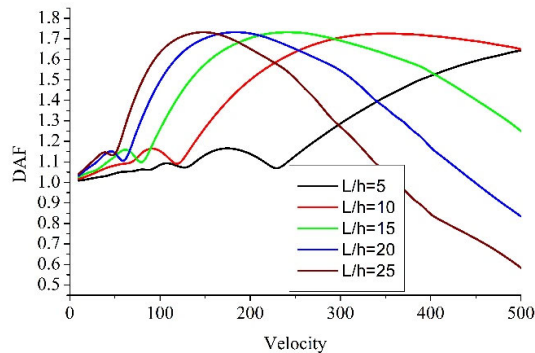


Figure 14 – Variation of the DAF as a function of  $L/h$  for  $k=1$ ,  $K_w=0$  and  $K_s=0$

The variation of the DAF of the FGM beam ( $k=1$ ) as a function of speed and slenderness  $L/h$  is shown in Figure 11. The factor is always maximal for longer beams. The maximum of this factor is almost the same (1.73) but at different speeds: 690 m/s for  $L/h=5$ , 360 m/s for  $L/h=10$ , 240 m/s for  $L/h=15$ , 190 m/s for  $L/h=20$  and 150 m/s for  $L/h=25$ .

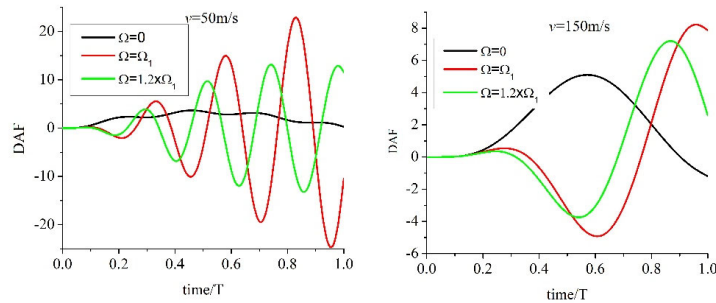


Figure 15 – Vibration of the mid-span section in relation to  $\Omega$  for  $v=50$  and  $v=150$  and  $K_w=0$  and  $K_s=0$

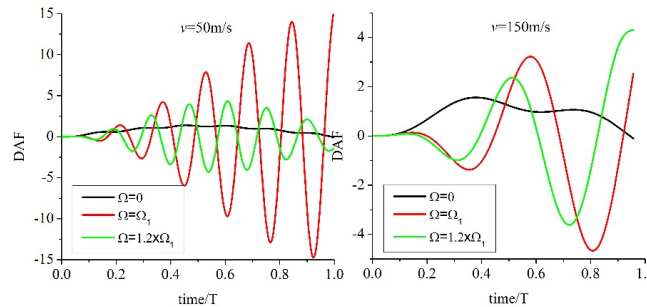


Figure 16 – Vibration of the mid-span section in relation to  $\Omega$  for  $v=50$  and  $v=150$  and  $K_w=100$  and  $K_s=10$

Figures 15 and 16 illustrate the phenomenon of resonance of an FGM beam ( $k=1$ ) for two speeds,  $v=50$  m/s and  $v=150$  m/s, with the foundation stiffnesses  $K_w=100$  and  $K_s=10$ . The moving load is harmonic, with a frequency that takes three values: 0,  $\Omega_1$  and  $1.2 \times \Omega_1$ , with  $\Omega_1$  being the fundamental frequency. The length of the beam is 10m,  $b=1$  m and  $L/h=15$ . The displacement values are multiplied by 1000. For a speed of 50 m/s, the amplitude of vibration reaches  $3.66 \times 10^3$  m, whereas the presence of excitation frequency, which is equal to the natural frequency, raises the amplitude to more than  $25 \times 10^3$  m and it continues to increase. The amplitudes in the case where  $\Omega = \Omega_1$  are 630% greater than in the case where  $\Omega=0$ . A frequency close to the natural frequency (20% greater) gives amplitudes ( $13.38 \times 10^3$  m) even much greater than in the case of zero frequency of excitation of the moving load. Increasing the speed to  $v=150$  m/s (Figure 14 (b)) induces amplitudes greater than in the case of zero frequency, but much less than in the first case where  $v=50$  m/s. The amplitudes in the  $\Omega = \Omega_1$  case are 58% greater than in the  $\Omega=0$  case. The presence of the elastic foundation causes a reduction in amplitudes.

## Conclusion

In the present work, a three-node finite element model using the higher-order shear deformation theory is developed to investigate the dynamic behavior of FGM beams under harmonic moving loads and elastic foundation support. By employing Hamilton's principle and the Galerkin method, we were able to derive the governing differential equations for the beam's behavior and effectively solve them. It has been shown in this article that the present finite element design is convergent, efficient and accurate, and that it is consistent with the results in the existing literature. The effects of various parameters on the free and forced vibration of FGM beams are also discussed. Our results underline the importance of taking the higher-order shear deformation theory into account in the dynamic analysis of FGM beams, thus providing a better understanding of their response to moving loads. This knowledge is essential for improving the design and performance of structures in various fields of engineering.

## References

- Barati, M.R., Faleh, N.M. & Zenkour, A.M. 2019. Dynamic response of nanobeams subjected to moving nanoparticles and hygro-thermal environments based on nonlocal strain gradient theory. *Mechanics of Advanced Materials and Structures*, 26(19), pp.1661-1669. Available at: <https://doi.org/10.1080/15376494.2018.1444234>.
- Barati, M.R. & Zenkour, A. 2018. Forced vibration of sinusoidal FG nanobeams resting on hybrid Kerr foundation in hygro-thermal environments. *Mechanics of Advanced Materials and Structures*, 25(8), pp.669-680. Available at: <https://doi.org/10.1080/15376494.2017.1308603>.
- Berrabah, H.M. & Boudierba, B. 2023. Mechanical buckling analysis of functionally graded plates using an accurate shear deformation theory. *Mechanics of Advanced Materials and Structures*, 30(22), pp.4652-4662. Available at: <https://doi.org/10.1080/15376494.2022.2102701>.
- Beskou, N.D. & Muho, E.V. 2018. Dynamic response of a finite beam resting on a Winkler foundation to a load moving on its surface with variable speed. *Soil Dynamics and Earthquake Engineering*, 109, pp.222-226. Available at: <https://doi.org/10.1016/j.soildyn.2018.02.033>.
- Chen, W.Q., Lü, C.F. & Bian, Z.G. 2004. A mixed method for bending and free vibration of beams resting on a Pasternak elastic foundation. *Applied Mathematical Modelling*, 28(10), pp.877-890. Available at: <https://doi.org/10.1016/j.apm.2004.04.001>.
- Chopra, A.K. 2014. *Dynamics of Structures: Theory and Applications to Earthquake Engineering, fourth edition*. Pearson. ISBN: 978-0-273-77424-2.
- Ebrahimi, F. & Jafari, A. 2018. A four-variable refined shear-deformation beam theory for thermo-mechanical vibration analysis of temperature-dependent

FGM beams with porosities. *Mechanics of Advanced Materials and Structures*, 25(3), pp.212-224. Available at: <https://doi.org/10.1080/15376494.2016.1255820>.

El Khouddar, Y., Adri, A., Outassafte, O., Rifai, S. & Benamar, R. 2023. An analytical approach to geometrically nonlinear free and forced vibration of piezoelectric functional gradient beams resting on elastic foundations in thermal environments. *Mechanics of Advanced Materials and Structures*, 30(1), pp.131-143. Available at: <https://doi.org/10.1080/15376494.2021.2009601>.

Esen, I. 2019. Dynamic response of a functionally graded Timoshenko beam on two-parameter elastic foundations due to a variable velocity moving mass. *International Journal of Mechanical Sciences*, 153-154, pp.21-35. Available at: <https://doi.org/10.1016/j.ijmecsci.2019.01.033>.

Esen, I., Eltaher, M.A. & Abdelrahman, A.A. 2023. Vibration response of symmetric and sigmoid functionally graded beam rested on elastic foundation under moving point mass. *Mechanics Based Design of Structures and Machines*, 51(5), pp.2607-2631. Available at: <https://doi.org/10.1080/15397734.2021.1904255>.

Fuchiyama, T. & Noda, N. 1995. Analysis of thermal stress in a plate of functionally gradient material. *JSAE Review*, 16(3), pp.263-268. Available at: [https://doi.org/10.1016/0389-4304\(95\)00013-W](https://doi.org/10.1016/0389-4304(95)00013-W).

Gan, B.S., Kien, N.D. & Ha, L.T. 2017. Effect of Intermediate Elastic Support on Vibration of Functionally Graded Euler-Bernoulli Beams Excited by a Moving Point Load. *Journal of Asian Architecture and Building Engineering*, 16(2), pp.363-369. Available at: <https://doi.org/10.3130/jaabe.16.363>.

Guo, L., Xin, X., Shahsavari, D. & Karami, B. 2022. Dynamic response of porous E-FGM thick microplate resting on elastic foundation subjected to moving load with acceleration. *Thin-Walled Structures*, 173, art.number:108981. Available at: <https://doi.org/10.1016/j.tws.2022.108981>.

Hasheminejad, S.M. & Rafsanjani, A. 2009. Three-Dimensional Vibration Analysis of Thick FGM Plate Strips Under Moving Line Loads. *Mechanics of Advanced Materials and Structures*, 16(6), pp.417-428. Available at: <https://doi.org/10.1080/15376490902781209>.

He, C., Zhu, J., Hua, Y., Xin, D. & Hua, H. 2023. A study on the vibration characteristics of functionally graded cylindrical beam in a thermal environment using the Carrera unified formulation. *Mechanics of Advanced Materials and Structures*, pp.1-13. Available at: <https://doi.org/10.1080/15376494.2023.2242861>.

Javidi, R., Rezaei, B. & Moghimi Zand, M. 2023. Nonlinear Dynamics of a Beam Subjected to a Moving Mass and Resting on a Viscoelastic Foundation Using Optimal Homotopy Analysis Method. *International Journal of Structural Stability and Dynamics*, 23(08), art.number:2350084. Available at: <https://doi.org/10.1142/S0219455423500840>.

Khalili, S.M.R., Jafari, A.A. & Eftekhari, S.A. 2010. A mixed Ritz-DQ method for forced vibration of functionally graded beams carrying moving loads. *Composite Structures*, 92(10), pp.2497-2511. Available at: <https://doi.org/10.1016/j.compstruct.2010.02.012>.

Le, T.H., Gan, B.S., Trinh, T.H. & Nguyen, D.K. 2014. Finite element analysis of multi-span functionally graded beams under a moving harmonic load. *Mechanical Engineering Journal*, 1(3), art.number:CM0013. Available at: <https://doi.org/10.1299/mej.2014cm0013>.

Li, Z., Xu, Y. & Huang, D. 2021. Analytical solution for vibration of functionally graded beams with variable cross-sections resting on Pasternak elastic foundations. *International Journal of Mechanical Sciences*, 191, art.number:106084. Available at: <https://doi.org/10.1016/j.ijmecsci.2020.106084>.

Lin, S.-M. & Lee, K.-W. 2016. Instability and vibration of a vehicle moving on curved beams with different boundary conditions. *Mechanics of Advanced Materials and Structures*, 23(4), pp.375-384. Available at: <https://doi.org/10.1080/15376494.2014.981618>.

Malekzadeh, P. & Monajjemzadeh, S.M. 2016. Dynamic response of functionally graded beams in a thermal environment under a moving load. *Mechanics of Advanced Materials and Structures*, 23(3), pp.248-258. Available at: <https://doi.org/10.1080/15376494.2014.949930>.

Menaa, R., Tounsi, A., Mouaici, F., Mechab, I., Zidi, M. & Bedia, E.A.A. 2012. Analytical Solutions for Static Shear Correction Factor of Functionally Graded Rectangular Beams. *Mechanics of Advanced Materials and Structures*, 19(8), pp.641-652. Available at: <https://doi.org/10.1080/15376494.2011.581409>.

Nguyen, V.D. & Phung, V.B. 2023. Static bending, free vibration, and buckling analyses of two-layer FGM plates with shear connectors resting on elastic foundations. *Alexandria Engineering Journal*, 62, pp.369-390. Available at: <https://doi.org/10.1016/j.aej.2022.07.038>.

Phadikar, J.K. & Pradhan, S.C. 2010. Variational formulation and finite element analysis for nonlocal elastic nanobeams and nanoplates. *Computational Materials Science*, 49(3), pp.492-499. Available at: <https://doi.org/10.1016/j.commatsci.2010.05.040>.

Praveen, G.N. & Reddy, J.N. 1998. Nonlinear transient thermoelastic analysis of functionally graded ceramic-metal plates. *International Journal of Solids and Structures*, 35(33), pp.4457-4476. Available at: [https://doi.org/10.1016/S0020-7683\(97\)00253-9](https://doi.org/10.1016/S0020-7683(97)00253-9).

Reddy, J.N. 2007. Nonlocal theories for bending, buckling and vibration of beams. *International Journal of Engineering Science*, 45(2-8), pp.288-307. Available at: <https://doi.org/10.1016/j.ijengsci.2007.04.004>.

Safaei, M., Malekzadeh, P. & Golbahar Haghighi, M.R. 2024. Out-of-plane moving load response and vibrational behavior of sandwich curved beams with GPLRC face sheets and porous core. *Composite Structures*, 327, art.number:117658. Available at: <https://doi.org/10.1016/j.compstruct.2023.117658>.

Saleh, B., Jiang, J., Fathi, R., Al-hababi, T., Xu, Q., Wang, L., Song, D. & Ma, A. 2020. 30 Years of functionally graded materials: An overview of manufacturing methods, Applications and Future Challenges. *Composites Part B: Engineering*, 201, art.number:108376. Available at: <https://doi.org/10.1016/j.compositesb.2020.108376>.

Şimşek, M. 2010. Vibration analysis of a functionally graded beam under a moving mass by using different beam theories. *Composite Structures*, 92(4), pp.904-917. Available at: <https://doi.org/10.1016/j.compstruct.2009.09.030>.

Şimşek, M. & Al-shujairi, M. 2017. Static, free and forced vibration of functionally graded (FG) sandwich beams excited by two successive moving harmonic loads. *Composites Part B: Engineering*, 108, pp.18-34. Available at: <https://doi.org/10.1016/j.compositesb.2016.09.098>.

Şimşek, M. & Kocatürk, T. 2009. Free and forced vibration of a functionally graded beam subjected to a concentrated moving harmonic load. *Composite Structures*, 90(4), pp.465-473. Available at: <https://doi.org/10.1016/j.compstruct.2009.04.024>.

Thai, H.-T. & Vo, T.P. 2012. Bending and free vibration of functionally graded beams using various higher-order shear deformation beam theories. *International Journal of Mechanical Sciences*, 62(1), pp.57-66. Available at: <https://doi.org/10.1016/j.ijmecsci.2012.05.014>.

Wang, X., Liang, X. & Jin, C. 2017. Accurate dynamic analysis of functionally graded beams under a moving point load. *Mechanics Based Design of Structures and Machines*, 45(1), pp.76-91. Available at: <https://doi.org/10.1080/15397734.2016.1145060>.

Xiang, S. & Kang, G.-W. 2013. A  $n$ th-order shear deformation theory for the bending analysis on the functionally graded plates. *European Journal of Mechanics - A/Solids*, 37(Jan-Feb), pp.336-343. Available at: <https://doi.org/10.1016/J.EUROMECHSOL.2012.08.005>.

Yan, T., Kitipornchai, S., Yang, J. & He, X.Q. 2011. Dynamic behaviour of edge-cracked shear deformable functionally graded beams on an elastic foundation under a moving load. *Composite Structures*, 93(11), pp.2992-3001. Available at: <https://doi.org/10.1016/j.compstruct.2011.05.003>.

Yan, T. & Yang, J. 2011. Forced Vibration of Edge-Cracked Functionally Graded Beams Due to a Transverse Moving Load. *Procedia Engineering*, 14, pp.3293-3300. Available at: <https://doi.org/10.1016/j.proeng.2011.07.416>.

Yang, J., Chen, Y., Xiang, Y. & Jia, X.L. 2008. Free and forced vibration of cracked inhomogeneous beams under an axial force and a moving load. *Journal of Sound and Vibration*, 312(1-2), pp.166-181. Available at: <https://doi.org/10.1016/j.jsv.2007.10.034>.

Yang, Y.B., Yau, J.D. & Wu, Y.S. 2004. *Vehicle-Bridge Interaction Dynamics: With Applications to High-Speed Railways*. World Scientific. Available at: <https://doi.org/10.1142/5541>.

Zemri, A., Houari, M.S.A., Bousahla, A.A. & Tounsi, A. 2015. A mechanical response of functionally graded nanoscale beam: an assessment of a refined nonlocal shear deformation theory beam theory. *Structural Engineering and Mechanics*, 54(4), pp.693-710. Available at: <https://doi.org/10.12989/sem.2015.54.4.693>.

Análisis dinámico forzado de vigas funcionalmente graduadas bajo cargas móviles armónicas sobre cimentación elástica con el método de elementos finitos

Amine Zemri<sup>a</sup>, **autor de correspondencia**, Ismail Mechab<sup>b</sup>

<sup>a</sup> Universidad de Relizane, Departamento de Ingeniería Civil y Obras Públicas, Relizane, República Argelina Democrática y Popular; Universidad de Sidi Bel Abbes, Laboratorio de Ingeniería Civil y Medio Ambiente, Sidi Bel Abbes, República Argelina Democrática y Popular

<sup>b</sup> Universidad de Sidi Bel Abbes, Departamento de Ingeniería Civil y Obras Públicas, Laboratorio de Estadística y Procesos Estocásticos, Sidi Bel Abbes, República Argelina Democrática y Popular

CAMPO: ingeniería mecánica, materiales

TIPO DE ARTÍCULO: artículo científico original

**Resumen:**

*Introducción/objetivo: Este artículo presenta un estudio numérico del comportamiento dinámico forzado de una viga funcionalmente graduada sometida a una fuerza de movimiento transversal concentrada que varía armónicamente utilizando una teoría de deformación cortante de orden superior.*

*Métodos: Las ecuaciones que rigen el problema se derivan utilizando el principio de Hamilton. Luego, estas ecuaciones se transforman en la forma débil utilizando el método de Galerkin. El problema se resuelve utilizando el método de elementos finitos mediante el desarrollo de un elemento finito de tres nodos con cuatro grados de libertad por nodo. Se elige el método beta de Newmark para la integración temporal y el método de Gauss para la integración espacial.*

*Resultados: Se investigaron los efectos de varios parámetros, entre ellos la relación de esbeltez, el índice de material, la rigidez de la cimentación, la velocidad y la frecuencia de la carga en movimiento. Se observó una buena concordancia con los resultados obtenidos de la bibliografía.*

*Conclusión: Este estudio ilustra la importancia de utilizar una teoría de orden superior en el caso de vigas cortas y muestra claramente el cambio en el comportamiento de la viga FGM en función de diferentes parámetros.*

*Palabras claves: teoría de deformación cortante de orden superior, material funcionalmente graduado, método de elementos finitos, carga móvil, método beta de Newmark.*

Анализ вынужденного динамического поведения функционально-градиентных балок при гармонической подвижной нагрузке на упругом основании методом конечных элементов

Амине Земри<sup>a</sup>, **корреспондент**, Исмаил Мечаб<sup>b</sup>

Zemri, A. et al, Forced dynamic analysis of functionally graded beams under harmonic moving loads on elastic foundation with the finite element method, pp.1272-1305



- <sup>a</sup> Университет Релизана,  
Факультет гражданского строительства и общественных работ,  
Релизан, Алжирская Народная Демократическая Республика;  
Университет Сиди-Бель-Аббеса,  
Лаборатория гражданского строительства и охраны окружающей среды,  
Сиди-Бель-Аббес, Алжирская Народная Демократическая Республика
- <sup>b</sup> Университет Сиди-Бель-Аббес, Факультет гражданского строительства и  
общественных работ, Лаборатория статистики и случайных процессов,  
Сиди-Бель-Аббес, Алжирская Народная Демократическая Республика

РУБРИКА ГРНТИ: 30.19.00 Механика деформируемого твердого тела,  
81.09.00 Материаловедение

ВИД СТАТЬИ: оригинальная научная статья

**Резюме:**

**Введение/цель:** В данной статье представлено численное исследование вынужденного динамического поведения функционально-градиентных балок под воздействием гармонически изменяющихся поперечных сил, с использованием теории сдвиговой деформации высокого порядка.

**Методы:** Управляющие уравнения получены с использованием принципа Гамильтона. Затем эти уравнения преобразованы в слабую форму с использованием метода Галеркина. Задача решается с использованием метода конечных элементов путем разработки трехузлового конечного элемента с четырьмя степенями свободы в узле. Для интегрирования по времени выбран бета-метод Ньюмарка, а для пространственного интегрирования – метод Гаусса.

**Результаты:** В статье было исследовано влияние нескольких параметров, включая коэффициент гибкости, индекс материала, жесткость основания, скорость и частоту перемещения нагрузки. Результаты исследования совпадают с результатами из научной литературы.

**Выводы:** Данное исследование иллюстрирует значимость теории высокого порядка в случае коротких балок и наглядно показывает изменение поведения функционально-градиентных балок в зависимости от различных параметров.

**Ключевые слова:** теория сдвиговой деформации высокого порядка, функционально-градиентный материал, метод конечных элементов, подвижная нагрузка, бета-метод Ньюмарка.

Анализа изазваног динамичког понашања функционално степенованих греда под хармоничним покретним оптерећењем на еластичној основи помоћу методе коначних елемената

Амин Земри<sup>а</sup>, аутор за преписку, Исмаил Мехаб<sup>б</sup>

<sup>а</sup> Универзитет у Релизану, Одељење за грађевинарство и јавне радове,  
Релизане, Народна Демократска Република Алжир;  
Универзитет Сиди Бел Абес,  
Лабораторија за грађевинарство и заштиту животне средине,  
Сиди Бел Абес, Народна Демократска Република Алжир

<sup>б</sup> Универзитет Сиди Бел Абес, Одељење за грађевинарство и јавне  
радове, Лабораторија за статистику и случајне процесе,  
Сиди Бел Абес, Народна Демократска Република Алжир

ОБЛАСТ: машинство, материјали

КАТЕГОРИЈА (ТИП) ЧЛАНКА: оригинални научни рад

**Сажетак:**

*Увод/циљ:* У раду је представљено нумеричко испитивање изазваног динамичког понашања функционално степеноване греде подвргнуте хармонично променљивој и трансферзално концентрисаној покретној сили уз коришћење теорије деформације смицањем вишег реда.

*Метод:* Најважније једначине изведене су помоћу Хамилтоновог принципа, а затим трансформисане у слаби облик помоћу методе Галеркина. Проблем је решен коришћењем методе коначних елемената путем развијања коначног елемента са три чвора од којих сваки има четири степена слободе. За интеграцију у времену изабрана је Њумаркова бета-метода, а за интеграцију у простору Гаусова метода.

*Резултати:* Испитан је утицај неколико параметара, укључујући виткост, индекс материјала и крутост, као и брзину и фреквенцију покретног оптерећења. Уочено је добро слагање са резултатима из литературе.

*Закључак:* Ово испитивање илуструје значај коришћења теорије вишег реда у случају кратких греда и јасно указује на промену у понашању функционално степеноване греде зависно од различитих параметара.

*Кључне речи:* теорија деформације смицањем вишег реда, функционално степенован материјал, метода коначних елемената, покретно оптерећење, Њумаркова бета-метода.

Paper received on: 02.04.2024.

Manuscript corrections submitted on: 24.09.2024.

Paper accepted for publishing on: 25.09.2024.

© 2024 The Authors. Published by Vojnotehnički glasnik / Military Technical Courier (www.vtg.mod.gov.rs, втг.мо.унр.срб). This article is an open access article distributed under the terms and conditions of the Creative Commons Attribution license (<http://creativecommons.org/licenses/by/3.0/rs/>).

